Reprinted from JOURNAL OF HEAT TRANSFER, Vol. 103, No. 1, February 1981

K.P. Singh
President and CEO
Holtec International

A Comparison of Thermal Performance of Two and Four Tube Pass Designs for Split Flow Shells

Governing equations for heat transfer in a split flow heat exchanger with two tube passes are developed and solved. The expressions for the "temperature efficiency" P and "LMTD temperature correction factor", F are derived. F and P values for two tube pass and four tube pass are compared over the practical range of values of thermal flow rate ratio R and reduced thermal flux, η (NTU).

Introduction

Split flow heat exchangers, designated as the "G-type" in TEMA standards [1] find extensive application in the process and power industries due to their relatively superior heat transfer and pressure drop characteristics. Schindler and Bates [2] present an excellent discussion on the merits of the split flow design over the conventional "E-type shell" construction.

They have also derived the relationships between the temperature efficiency P, reduced thermal flux η and thermal flow rate ratio R for split flow, two tube pass heat exchanger. Singh and Holtz [3] presented similar relationships for split flow, four tube pass exchanger. Although the relationships for four tube pass and two tube pass cases are mathematically completely different, one would suspect from physical reasoning that their actual performances may not be so dissimilar. One of the objectives of this paper is to compare the heat transfer performance of two and four tube pass arrangements in the meaningful range of the governing dimensionless parameters. Another goal in this paper is to derive heat transfer expressions for a split flow, two tube pass heat exchanger. This entails determining tube and shell side fluid temperatures as functions of the surface area coordinate; and of course, the relationships between P, η and R. Schindler and Bates [2] obtain these relationships by dividing the heat transfer region into two concurrent and one countercurrent subregion. They utilize integrated heat transfer relations for each subregion in terms of (as yet undetermined) terminal temperatures; and appeal to temperature continuity across inter-subregion boundaries to determine the unknown terminal temperatures. Further manipulation of the mathematical expressions yields the desired relationships among P, η and R. The approach presented in this paper, on the other hand, is based on the first principles. Fundamental heat transfer relations for a differential element in a subregion are written. The resulting differential equations are integrated. The constants of integration are found using temperature continuity across subregion interfaces. In this manner, the overall characteristics as well as details of the temperature field are determined. The knowledge of the temperature profiles of the tubeside and shellside streams is essential in many design calculations. For example, the computation of tube/shell longitudinal stress in fixed tubesheet heat exchangers and U-bend stress in U-tube exchangers [4] require evaluation of the total longitudinal expansion of the tubes. Temperature profiles also reveal regions of inadequate or reverse heat transfer [3], locations of possible high thermal stress in the tubesheet, etc. In view of these considerations, the formulation in this paper seeks to synthesize the overall apparatus response from the elemental relationships. The difference from the Schindler, et al. solution is not so much in the conceptual approach as it is in the methodology. The thermal-hydraulic assumptions implied in the analysis are the traditional ones listed in reference [3] from (*a*) to (*g*) (excluding (*h*)). A brief description of the analysis now follows.

Contributed by the Heat Transfer Division for publication in the JOURNAL OF HEAT TRANSFER. Manuscript received by the Heat Transfer Division, March 21, 1980.

Analysis

As shown in Fig. 1, the shell side stream enters the shell at the shell nozzle located midway along the shell. The shell stream subdivides into two equal substreams flowing in opposite directions in the upper half of the shell. Having traversed the two extremities of the shell, these two substreams cross over the longitudinal baffle and flow towards the outlet nozzle located midway along the shell length in the bottom half of the shell. The heat transfer region is subdivided into three subregions as indicated in Fig. 1. If A_i is used to denote the surface area on tubes in subregion i, then we note that $A_1 = A_3 = 0.25A^*$; and $A_2 = 0.5A^*$, where A^* is the overall heat transfer surface. To fix ideas, we set up a coordinate system in each subregion such that the origin of the coordinate A (tube surface area) is located in the plane where the shell side fluid enters the subregion, and the magnitude of A increases in the direction of the shell side flow. Thus the origin of surface area parameter A in subregion 3 is at the left-hand tube sheet in Fig. 1. Noting that the shell side and tube side flows are cocurrent in subregions 1 and 3, and countercurrent in subregion 2, the following heat transfer relations can be readily written:

$$0.5M_s\delta_i dT = M_t dt;\ i = 1, 2, 3 \tag{1}$$

$$0.5M_s dT = -U(T - t)dA \tag{2}$$

Where M_s and M_t are shell side and tube side thermal flow rates, U is the overall heat transfer coefficient, T and t denote shellside and tubeside fluid temperatures at a typical elemental surface dA defined by surface coordinate location A. δ_i characterizes the flow pattern

$$\delta_i = (-1)^i \tag{2a}$$

From equation (2), we have

$$\frac{dT}{dA} = \frac{-2U}{M_s}(T - t) \tag{3}$$

or

$$\frac{d^2T}{dA^2} = \frac{-2U}{M_s}\left(\frac{dT}{dA} - \frac{dt}{dA}\right) \tag{4}$$

Substituting for dt/dA from equation (1), we obtain a second order differential equation in T

$$\frac{d^2T}{dA^2} + \alpha_i \frac{dT}{dA} = 0;\ i = 1, 2, 3 \tag{5}$$

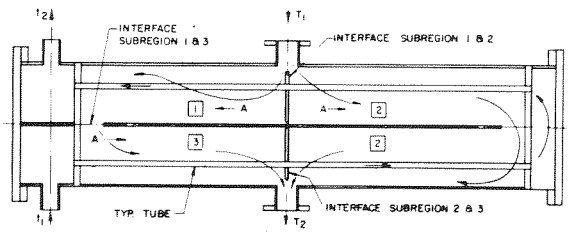

Fig. 1 Schematic of split flow, two pass heat exchanger

where

$$\alpha_i = \frac{2U}{M_s}\left(1 - \frac{\delta_i}{2R}\right) \tag{6}$$

and R is the ratio of thermal flow rate on the tube side to that on the shell side; i.e.,

$$R = \frac{M_t}{M_s} \tag{6a}$$

Solution of equation (5) yields

$$T = a_i + b_i e^{-\alpha_i A};\ i = 1, 2, 3 \tag{7}$$

This yields, together with equation (3)

$$t = a_i + b_i\left(1 - \frac{M_s\alpha_i}{2U}\right)e^{-\alpha_i A};\ i = 1, 2, 3 \tag{8}$$

The special case where $\alpha_i = 0$ is treated separately later in this section. Six constants of integration, a_i, b_i are evaluated by using interface conditions between the subregions and the boundary conditions, as follows.

(i) Between subregions 1 and 2, ($A = 0$) continuity in T requires

$$a_1 + b_1 = a_2 + b_2 \tag{9}$$

(ii) Similarly, continuity in t requires (at $A = 0$)

$$a_1 + b_1\left(1 - \frac{M_s\alpha_1}{2U}\right) = a_2 + b_2\left(1 - \frac{M_s\alpha_2}{2U}\right) \tag{10}$$

From equations (9) and (10) we have

$$b_2 = \frac{\alpha_1}{\alpha_2}b_1 \tag{11}$$

$$a_2 = a_1 + b_1\left(1 - \frac{\alpha_1}{\alpha_2}\right) \tag{11a}$$

(iii) At the interface between subregions 1($A = A_1$) and 3($A = 0$), continuity of T yields

$$a_1 + b_1\theta_1 = a_3 + b_3 \tag{12}$$

where

$$\theta_i = e^{-\alpha_i A_i} \tag{12a}$$

(iv) Continuity of tube side fluid temperature at the interface between subregion 2($A = A_2$) and subregion 3($A = A_3$) yields

$$a_3 + b_3\theta_3\left(1 - \frac{M_s\alpha_3}{2U}\right) = a_2 + b_2\theta_2\left(1 - \frac{M_s\alpha_2}{2U}\right) \tag{13}$$

Substituting for a_2 and b_2 from equations (11), (11a) and (13), we have

$$a_3 + b_3\theta_3\left(1 - \frac{M_s\alpha_3}{2U}\right) = a_1 + b_1\left[1 - \frac{\alpha_1}{\alpha_2} + \frac{\theta_2\alpha_1}{\alpha_2}\left(1 - \frac{M_s\alpha_2}{2U}\right)\right] \tag{13a}$$

From equations (12) and (13a), we have

$$b_3 = \chi b_1 \tag{14}$$

where

$$\chi = \frac{1 - \theta_1 - \frac{\alpha_1}{\alpha_2} + \frac{\theta_2\alpha_1}{\alpha_2}\left(1 - \frac{M_s\alpha_2}{2U}\right)}{\theta_3\left(1 - \frac{M_s\alpha_3}{2U}\right) - 1} \tag{15}$$

Furthermore, equation (12) gives

$$a_3 = a_1 + b_1(\theta_1 - \chi) \tag{16}$$

Finally, two boundary conditions may be specified as

(v) $T = T_1$ at $A = 0$ in subregion 1.

(vi) $t = t_1$ at $A = 0$ in subregion 3.

From equations (7) and (8), we obtain using the above condition:

$$T_1 = a_1 + b_1 \tag{17}$$

$$t_1 = a_1 + b_1\left(\theta_1 - \frac{\chi\alpha_3 M_s}{2U}\right) \tag{18}$$

Hence

$$T_1 - t_1 = b_1\left(1 - \theta_1 + \frac{\chi\alpha_3 M_s}{2U}\right)$$

or

$$b_1 = \frac{(T_1 - t_1)}{1 - \theta_1 + \frac{\chi\alpha_3 M_s}{2U}} \tag{19}$$

Finally

$$a_1 = \frac{T_1\left(\frac{\chi\alpha_3 M_s}{2U} - \theta_1\right) + t_1}{1 - \theta_1 + \frac{\chi\alpha_3 M_s}{2U}} \tag{20}$$

Thus all the constants of integration are expressed in terms of input data, and the temperature profiles of both shellside and tubeside fluids become completely known.

It is of some interest to derive the relationship between temperature efficiency P, reduced thermal flux η and thermal flow rate ratio R where these nondimensional quantities are defined in terms of previously introduced terms as follows.

$$P = \frac{t_2 - t_1}{T_1 - t_1} \quad (a)$$

$$\eta = \frac{UA^*}{M_t} \quad (b) \tag{21}$$

R is defined by equation (6a).

Noting that the tube outlet temperature t_2 is given by the subregion 1 solution for t at $A = A_1$, we have

$$t_2 = a_1 + b_1\theta_1\left(1 - \frac{M_s\alpha_1}{2U}\right) \tag{22}$$

Equations (18) and (22) yield

Nomenclature

A^* = overall heat transfer surface
A_i = heat transfer surface in subregion i
a_i, b_i = constants of integration in subregion i
A = surface area coordinate in a subregion with reference to its local coordinate system (Fig. 1)
F_4, F_2 = LMTD correction factor for split flow four-tube pass and two-tube pass exchangers, respectively
M_s = thermal flow rate of shellside fluid
M_t = thermal flow rate of tubeside fluid
P = temperature efficiency (equation (21a))
P_4, P_2 = temperature efficiency of four-tube pass and two-tube pass (split flow) exchanger, respectively
R = thermal flow rate (flow rate times specific heat) ratio (equation (6a))
U = overall heat transfer coefficient
T = shellside fluid temperature at a generic surface coordinate A
t = tubeside fluid temperature of a generic surface coordinate A
t_1 = tube inlet temperature
t_2 = tube outlet temperature
T_1 = shell inlet temperature
T_2 = shell outlet temperature
η = number of transfer units (also referred to as reduced thermal flux in this paper) equation (21b)

$$t_2 - t_1 = b_1\left(\frac{\chi\alpha_3 M_s}{2U} - \frac{M_s\alpha_1\theta_1}{2U}\right) \tag{23}$$

The expression for P now follows from equations (19) and (23)

$$P = \frac{t_2 - t_1}{T_1 - t_1} = \frac{\frac{M_s}{2U}(\chi\alpha_3 - \alpha_1\theta_1)}{1 - \theta_1 + \frac{\chi\alpha_3 M_s}{2U}} \tag{24}$$

or

$$P = \frac{\frac{2}{\eta R}(\theta_1 \ln\theta_1 - \chi \ln\theta_3)}{1 - \theta_1 - \frac{2\chi \ln\theta_3}{\eta R}} \tag{25}$$

θ_1 and χ can be readily expressed in terms of dimensionless quantities, as follows.

$$\theta_1 = \theta_3 = \frac{-\eta R}{e^2}\left(1 + \frac{1}{2R}\right) \qquad (a)$$

$$\theta_2 = e^{-\eta R}\left(1 - \frac{1}{2R}\right) \qquad (b) \tag{26}$$

$$\chi = \frac{1 - \theta_1 - \frac{2\ln\theta_1}{\ln\theta_2} + \frac{2\theta_2 \ln\theta_1}{\ln\theta_2}\left(1 + \frac{\ln\theta_2}{\eta R}\right)}{\theta_3\left(1 + \frac{2\ln\theta_3}{\eta R}\right) - 1} \qquad (c)$$

All necessary heat transfer relations are now available in terms of the conventional dimensionless parameters.

Special case: Referring to equation (6), $R = 0.5$ makes α_2 zero. For this case the governing equation (equation (5)) becomes for $i = 2$

$$\frac{d^2T}{dA^2} = 0 \tag{27}$$

which is integrated to yield

$$T = a_2 + b_2 A \tag{28}$$

The corresponding expression for the tubeside fluid temperature follows from equation (8)

$$t = a_2 + b_2\left(A + \frac{M_s}{2U}\right) \tag{29}$$

Using the boundary conditions as before, the following relationships between the constants of integration follow:

$$\begin{aligned} a_2 &= a_1 + b_1 \\ b_2 &= -\alpha_1 b_1 \\ b_3 &= \chi b_1 \end{aligned} \tag{30}$$

where

$$\chi = \frac{1 - \theta_1 + 2\ln\theta_1\left(1 + \frac{1}{\eta R}\right)}{\theta_3\left(1 + \frac{2\ln\theta_3}{\eta R}\right) - 1} \tag{31}$$

The expressions for P (equation (25)), b_1 (equation (19)), a_1 (equation (20)) remain unchanged.

Temperature Correction Factor

Equations (25) and (26) completely characterize the heat transfer behavior of two tube pass split flow heat exchanger. For a given value of η and R the temperature efficiency P is readily evaluated. Thus the well-known ten Broeck Charts can be conveniently constructed for this geometry. Furthermore, the log mean temperature difference correction factor, (LMTD) F, can be computed using the basic relationship

$$F = \frac{\ln\frac{1-P}{1-PR}}{\eta(R-1)} \tag{32}$$

It should be noted that the above equation shows F to be an explicit function of three variables, namely η, P and R. P can be expressed in terms of η and R using equation (25); thus F becomes a function of η and R only. In principle it is possible to express η in terms of P and R by rearranging and manipulating equation (25) and thus render F to be a function of P and R, which is the most common form of representation in the so-called "temperature correction factor" charts. However, η is a highly complex function of P and R, requiring an iterative solution to compute η for given values of P and R. It is most convenient to generate P for selected values of η and R (using equation (25)) and then proceed to compute F using equation (32). The design charts are thus generated for practical use. Schindler and Bates [2] published such charts for the two pass split flow heat exchanger; hence, these are not presented here. It is, however, of some interest to examine how the LMTD correction factor, F, and temperature efficiency P compare for two and four tube pass split flow geometries. The values of P and F are calculated for four tube pass using the Singh and Holtz [3] solution. The differences ΔP and ΔF are plotted as functions of η (with R as the parameter) in Figs. 2 and 3 where

$$\Delta P = P_2 - P_4; \text{ and } \Delta F = F_2 - F_4$$

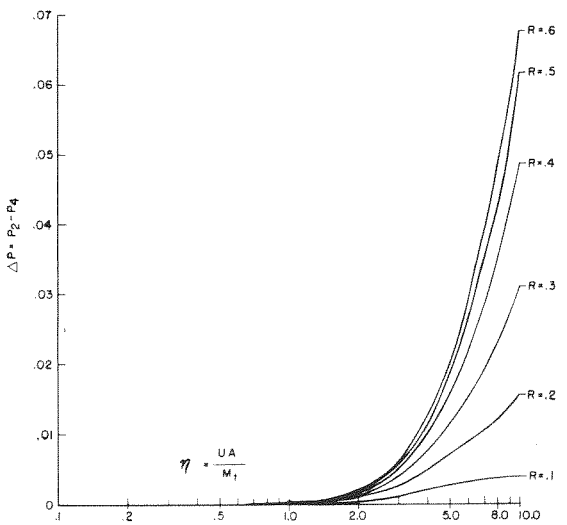

Fig. 2 Differential temperature efficiency versus reduced thermal flux (NTU)

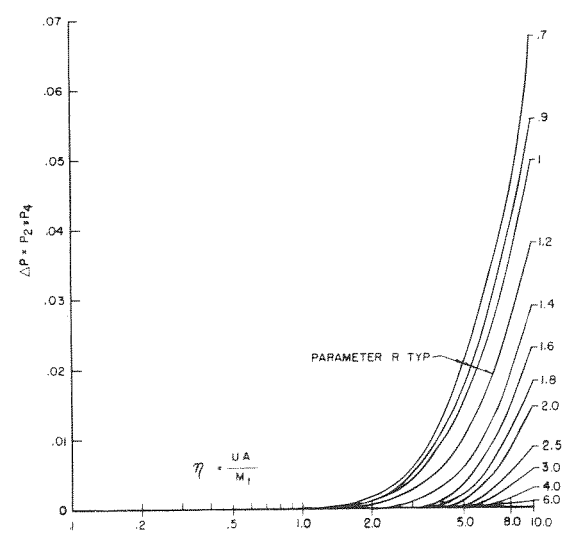

Fig. 3 Differential temperature efficiency versus reduced thermal flux (NTU)

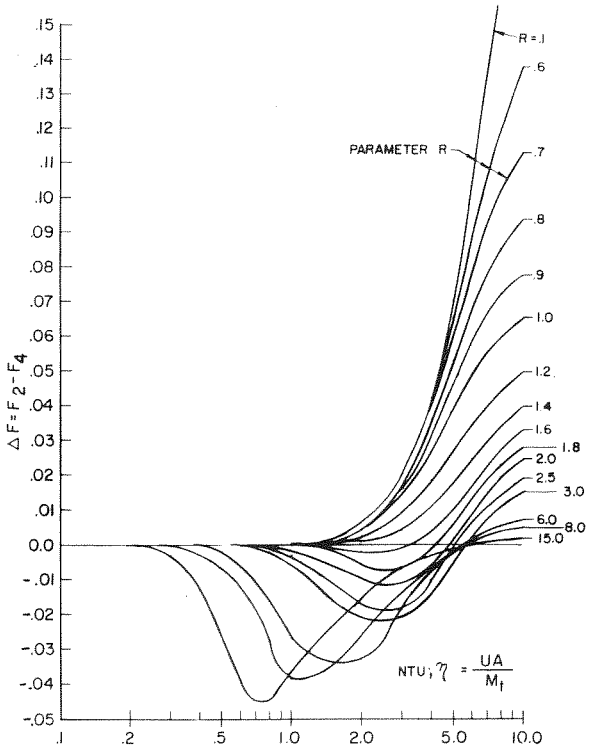

Fig. 4 Differential temperature correction factor ΔF versus NTU

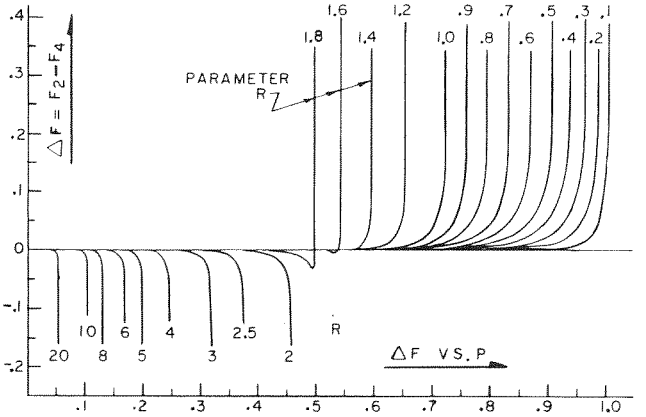

Fig. 5 Temperature efficiency, *P*

The plots for ΔP (Figs. 2 and 3) show that the difference in temperature efficiency is highest around $R = 0.7$, and decreases rather rapidly for greater or smaller values of R. ΔP is also seen to be a monotonically increasing function of η. ΔF is plotted versus η in Fig. 4 with R as parameter. Greater values of ΔF appear to correspond with large η and small R. In the most meaningful design range, however ($\eta < 3$), we notice that ΔF is less than 0.05. Thus the thermal performance of the two geometries is nearly equal in this range. Figure 5 shows ΔF as a function of P. Thus, Fig. 5 may be used to determine the relative efficacies of two and four pass geometries directly from the input data usually available (P and R). The following conclusions may be drawn from the foregoing discussion:

1 Two and four pass split flow designs have nearly identical operating performance characteristics in the meaningful design range.

2 Two pass design has a performance edge over four pass for relatively small R (<1.6). Four pass design becomes increasingly more efficient for greater R (Fig. 4). This fact is further borne out by Fig. 5. However, four tube pass design may not be suitable for high R values due to tubeside pressure drop limitations.

3 The figures presented here should enable a practicing engineer to make rapid comparison between two and four (or more) pass configurations for his particular problem.

4 It can be deduced from the foregoing that in the meaningful range of design data, six and more pass geometries will behave likewise. Thus the temperature performance curves for two pass and four pass currently available can be used to predict the performance of multipass designs with satisfactory accuracy.

Acknowledgment

The authors are thankful to Dr. Jerry Taborek of HTRI for his thoughtful comments on this paper during its preparation.

References

1 *Standards of Tubular Manufacturer's Association*, Sixth edition, New York, 1978, p. 3.

2 Schindler, D. L., and Bates, H. T., "True Temperature Difference in a 1-2 Divided-Flow Heat Exchanger," *Chemical Engineering Progress Symposium*, Series No. 30, Vol. 56, 1960, pp. 203–206.

3 Singh, K. P., and Holtz, M. J., "Generalization of the Split Flow Heat Exchanger Geometry for Enhanced Heat Transfer," *AIChE Symposium Series*, No. 189, Vol. 72, 1979, pp. 219–226.

4 Singh, K. P., and Holtz, M., "On Thermal Expansion Induced Stresses in U-Bends of Shell-and-Tube Heat Exchangers," ASME *Journal of Engineering for Power*, Vol. 101, No. 4, 1979, pp. 634–639.